

Published in final edited form as:

Dev Dyn. 2011 July ; 240(7): 1745–1755. doi:10.1002/dvdy.22674.

The Abelson tyrosine kinase is required for *Drosophila* photoreceptor morphogenesis and retinal epithelial patterning

Wenjun Xiong and Ilaria Rebay¹

Ben May Department for Cancer Research, The University of Chicago, 929 E57th St., Chicago, IL 60637, USA

Abstract

Coordinated differentiation and morphogenesis transform the *Drosophila* retina from a layer of epithelial cells into a complex three-dimensional organ. In this study we show that the Abelson (Abl) tyrosine kinase localizes to the dynamically remodeling apical-junctional membrane domains of the developing photoreceptors cells. Analyses of *abl* mutant clone phenotypes demonstrate that *abl* is required for enriched localization of adherens junction and apical polarity complex proteins at photoreceptor-photoreceptor cell junctions and apical membrane domains, respectively, for rhabdomere generation and for spatial organization of ommatidial cells along the apical-basal axis of the epithelium. Loss of *abl* does not alter expression or localization of Enabled (Ena) nor does heterozygosity for *ena* dominantly suppress the *abl* phenotypes, suggesting the downstream effector mechanisms used by Abl in the eye may differ from those used in the embryo. Together our results reveal a prominent role for Abl in coordinating multiple aspects of photoreceptor morphogenesis.

Introduction

The *Drosophila* compound eye provides a powerful model for elucidating the genetic circuitries that coordinate cellular proliferation, differentiation and morphogenesis during epithelial patterning and organogenesis. Retinal development begins in the first instar larval eye imaginal disc, a simple monolayer of proliferating cells. At the third instar stage, coordinated apical constriction produces a dorsoventrally aligned indentation in the epithelium, referred to as the morphogenetic furrow (MF). As the MF crosses the eye disc, cells are arrested in G1 and recruited in a stereotyped sequence into the developing ommatidia. R8 photoreceptor cells are specified first, followed sequentially by photoreceptors R2/5, R3/4, R1/6, R7, the cone cells and finally the pigment cells (for a review, see Kumar and Moses, 2000). After their fates are designated, dramatic morphogenetic changes accompany the differentiation program as each cell type assumes its appropriate shape and position. Thus cell-cell contacts and structures that initiate in an essentially two-dimensional epithelial sheet elaborate to organize the tissue into a three-dimensional organ while in parallel, specific morphogenetic programs produce the distinct structural characteristics of each cell type.

Morphogenesis and patterning of the *Drosophila* retina have been extensively described (Tomlinson and Ready, 1987 and Fig. 1A; Cagan and Ready, 1989; Longley and Ready, 1995). Briefly, as photoreceptors are recruited into the developing ommatidial clusters, enrichment of adherens junction (AJ) proteins at the apical junctional region stabilizes essential cell-cell contacts that both organize intercellular signaling and provide structural

¹To whom correspondence should be addressed.

scaffolds for morphogenesis and ommatidial patterning (Gibson and Perrimon, 2003; Tepass and Harris, 2007). Shortly after specification of the four cone cells, the apical membranes and AJs of the photoreceptors involute and turn 90° toward the center of each ommatidium, followed by a massive expansion perpendicular to the epithelium plane (Longley and Ready, 1995). Beginning at approximately 35 hours after puparium formation (APF), specialization of the apical domain and subsequent elongation of the photoreceptors generates the extended rod-like rhabdomeres, which are packed with actin filament-enriched microvilli. By the mid-pupal stage, after all accessory cells are recruited, cells within each ommatidium adopt a stereotypic three dimensional arrangement as a result of differential cell adhesions (Hayashi and Carthew, 2004). For each ommatidial unit, eight photoreceptors form an inner circle surrounded by four cone cells and eleven pigment cells organized into two outer whorls (Ready et al., 1976). Along the apical-basal axis, the photoreceptors cells occupy the middle of the epithelium, with the cell bodies of the cone cells and pigment cells above and below, respectively.

Although the morphogenetic events that pattern the *Drosophila* retinal epithelium are well-characterized, the signaling networks that organize and coordinate these dynamic processes remain relatively poorly understood. Therefore, investigating the functions of conserved signaling molecules that direct changes in cytoskeleton dynamics, intercellular junctions and apicobasal polarity during photoreceptor development should provide a powerful strategy for elucidating the molecular mechanisms that drive cellular morphogenesis and epithelial patterning, not only in the *Drosophila* eye, but also in other stratified epithelia.

Drosophila abelson (abl), homolog of the vertebrate c-abl oncogene, encodes a widely expressed cytoplasmic tyrosine kinase that influences a variety of morphogenetic processes through regulation of the actin cytoskeleton. For example, in the embryonic central nervous system (CNS), Abl transduces signals from several axon guidance receptors to the cortical actin cytoskeleton via interactions with the actin modulator Enabled and the guanine nucleotide-exchange factor Trio (Bashaw et al., 2000; Liebl et al., 2000; Forsthoefel et al., 2005). In embryonic epithelia, loss of *abl* compromises AJ stability, actin organization and apical constriction (Grevengoed et al., 2001; Grevengoed et al., 2003; Fox and Peifer, 2007). While much of Abl's regulation of actin organization occurs by antagonizing the function and localization of Enabled (Grevengoed et al., 2003; Fox and Peifer, 2007), Abl may also directly influence actin organization via its C-terminal F- and G-actin binding domains (Hernandez et al., 2004). Although its function in fly eye development has not been extensively examined, Abl is expressed in the developing photoreceptors, is required for normal eye development, and has recently been implicated in photoreceptor axon targeting and planar cell polarity (Bennett and Hoffmann, 1992; Xiong et al., 2009), suggesting it might play an important role in the signaling networks directing terminal differentiation and morphogenesis of these cells.

In this study, we examine the role of Abl in patterning the *Drosophila* retina by analyzing *abl* loss-of-function clonal phenotypes in larval and pupal eye imaginal discs. Consistent with Abl's dynamic subcellular localization during photoreceptor apical membrane and AJ remodeling, loss of *abl* leads to defects in the photoreceptor AJs and apical membrane domains, and a subsequent failure to maintain the relative position of the photoreceptor cell bodies along the apicobasal axis of the retinal epithelium. Apical and cortical F-actin appear normal in *abl* mutant photoreceptors before 24hr APF, after which there is a striking absence of F-actin accumulation at the apex of the photoreceptor apical membranes, and an ensuing failure of rhabdomere biogenesis. In contrast to previous investigations of Abl function in *Drosophila* embryonic epithelia, Enabled (Ena) localization is not altered in *abl* clones, nor does genetic reduction of *ena* suppress the morphogenetic defects seen in *abl* mutant photoreceptors. Thus we propose that Abl is a key regulator of photoreceptor morphogenesis

and retinal epithelial patterning, and that the downstream signaling mechanisms may not be identical to those used in the embryo.

Results

Dynamic localization of Abl at the regionalizing apical membrane domains of the developing photoreceptors

As the first step of our study to understand Abl function in the retinal epithelium, we examined its expression pattern and subcellular localization in developing eye imaginal discs. The onset of prominent Abl expression in the photoreceptor clusters occurs a few rows posterior to the morphogenetic furrow (Bennett and Hoffmann, 1992 and Fig. 1B), coincident with the refinement of the apical surface marker atypical protein kinase C (aPKC) localization into discrete foci at the center of each developing cluster (Fig. 1B' & B'''). Examination of subcellular localization along the apical-basal axis shows enrichment of Abl at the constricting apical membranes of the photoreceptors in a domain that colocalizes with aPKC at the most apical plane and extends subapically into the AJ region marked by Armadillo (Arm) (Fig. 1C-E). Less prominent Abl accumulation is seen along the basolateral membranes (Fig. 1C and 1F). Consistent with Abl's key roles in regulating the actin cytoskeleton during embryonic epithelial development (Grevengoed et al., 2001; Grevengoed et al., 2003; Fox and Peifer, 2007), Abl also overlaps with apical filamentous actin (F-actin) (Fig. 1F).

By mid-pupal stage (48hr APF), the photoreceptor apical membranes have involuted toward the center of each ommatidial cluster and are becoming specialized into two subdomains, the central rhabdomeres and the surrounding stalk membranes that connect the rhabdomere to the AJs. Thus, we asked whether Abl distribution becomes refined to a particular domain during this apical membrane remodeling process or whether it remains broadly localized across all apical structures. Comparison of Abl localization to that of the rhabdomere marker F-actin, the stalk membrane marker aPKC and the AJ marker Arm at 48hr APF shows that Abl is concentrated in the center of each ommatidium together with F-actin, partially colocalizes with aPKC, and does not overlap with Arm (Fig. 1G-L). The restriction of Abl to the F-actin rich rhabdomere domain positions Abl appropriately to direct cytoskeletal changes that drive apical membrane expansion and specialization during rhabdomere formation, while its broader localization at third instar suggests an earlier role in establishing the apical membrane domain and cellular junctions.

Abl is required for the organization of the photoreceptor apical membrane domain and adherens junctions

To test whether Abl is essential for the establishment and/or maintenance of the photoreceptor apical membrane domain and AJs, we used the *eyeless*-FLP/FRT system (Newsome et al., 2000a) to generate mosaic clones of an *abl*² null allele and then compared expression and localization of relevant markers in the mutant (marked by the absence of GFP) versus wild-type (GFP-positive) tissue. To rule out genetic background effects, phenotypes were confirmed in clones of *abl*¹, a strong hypomorph. We first examined the consequences of *abl* loss on the photoreceptor AJs by following expression of Arm. In third instar *abl* mutant clones, the intense enrichment of Arm protein seen in wild-type ommatidia at the intercellular junctions between differentiating photoreceptors appears reduced, although fairly normally patterned, suggesting a defect or delay in AJ specialization (Fig. 2A, D-E and Supp. Fig. 2A). At 24hr APF, the AJs between the four cone cells are normal in *abl* mutant ommatidia (Fig. 2F), consistent with our observation that Abl does not appear to be expressed in the cone or other accessory cell types (data not shown). However, junctional Arm appears less tightly organized between *abl* mutant photoreceptor cells (Fig. 2B, G-H).

At 48hr APF, as the AJs of the photoreceptors extend along the growing apical domain perpendicularly to the retinal epithelial surface, Arm staining reveals the stereotyped AJ pattern of seven dots in transverse sections of wild-type ommatidia (Fig. 2C, I and Supp. Fig. 2B). In *abl* mutant ommatidia, Arm staining is no longer detected apically, but can be found collapsed to the basal plane (Fig. 2C, J, K), suggesting a gross disruption in epithelial organization.

We next investigated the consequences of loss of *abl* on apical membrane establishment and maintenance by examining the expression of three apical markers, aPKC, Crumbs and PATJ, in *abl* mutant photoreceptors. Similar to Arm staining, the normally strong accumulation of these three apical surface markers in the center of each ommatidial cluster was greatly reduced in third instar *abl* mutant clones (Fig. 3A-I). By 48hr APF, normal levels of the apical surface markers were restored in the *abl* mutant photoreceptors, but were detected at the basal plane of the epithelium (Fig. 3J-U). Together these results suggest a role for Abl in organizing and stabilizing the apical membrane domains and AJs of the photoreceptor cells.

Loss of *abl* alters the apicobasal distribution of the photoreceptors

The collapse of both AJ and apical surface markers to the basal plane of the epithelium raises the possibility of altered apicobasal positioning of photoreceptor cells within *abl* mutant ommatidia. Using the pan-neuronal marker Elav to follow nuclear position, we analyzed the apicobasal arrangement of *abl* mutant photoreceptors in larval and pupal eye discs. In wild type, as cells are recruited to join the developing ommatidial cluster, both their nuclei and cell bodies rise apically to establish their proper place within the epithelium (Tomlinson, 1985). However, at the third instar larval stage, some *abl* mutant clusters reside slightly basal to their wild type neighbors (Fig. 4A). Arguing that this is not simply a developmental delay in photoreceptor recruitment and apical migration, as the retinal cells elongate perpendicular to the plane of the epithelium during pupal development, the altered apicobasal positioning of the photoreceptor nuclei becomes more apparent (Fig. 4B-C and Supp. Fig. 3). Quantification of this phenotype in 154 *abl* mutant ommatidia in five different 48hr APF discs revealed an average of only 1.5 Elav-positive nuclei remaining at the normal apical plane, with the rest collapsing basally.

By 48hr APF, the specification and spatial organization of all retinal cells in a wild type eye imaginal disc has been accomplished, with different cell types occupying distinct geometric positions along the apical-basal axis such that the lens-secreting cone cell nuclei are at the apical planes of the epithelium, the photoreceptor nuclei are in the middle and the pigment cell nuclei are at the bottom (schematized in Fig. 4F). To determine both the extent of overall ommatidial disorganization and where the basally displaced *abl* mutant photoreceptor nuclei reside relative to the cone and pigment cell nuclei in 48hr APF mosaic eye discs, we examined the expression of the photoreceptor cell marker Elav and the transcription factor Sine oculis (So), which is expressed strongly in cone and more weakly in pigment cells. In wild-type ommatidia, expression of these two markers reveals the apical to basal positioning of the nuclei of the four cone cells, the eight photoreceptor cells and the twelve pigment cells (Fig. 4D). Although *abl* mutant ommatidia have apically positioned So-positive cone cell nuclei (Fig. 4E), the relative apicobasal positioning of the other cell types is altered such that the photoreceptor cell nuclei that normally reside between the cone and pigment cells fall basally to the pigment cell nuclei (Fig. 4E, and schematized in Fig. 4F). Examination of Choptin expression, which outlines the photoreceptor cell membrane, further confirms the disrupted apicobasal distribution of *abl* mutant photoreceptor cell bodies (Supp. Fig. 1).

What happens to apical-basal organization in mosaic ommatidia that contain a mix of *abl* mutant and wild-type photoreceptors? In cases where a single *abl* mutant photoreceptor is contacted by two wild-type neighboring cells, the mutant cell nucleus always resides properly at the apical plane and junctional Arm expression between mutant and wild-type cells appears normal (Fig. 4G). Even with two or three adjacent *abl* mutant cells, as long as the majority of photoreceptors in the mosaic ommatidium are wild-type, the apicobasal position of and the Arm staining between the mutant cells appears normal (Fig. 4G). Thus the presence of wild-type photoreceptors within an ommatidium can non-autonomously rescue the apical-basal position and junctional organization defects associated with *abl* loss.

Apical and cortical F-actin organization appear unaffected by loss of *abl* in larval and early pupal photoreceptors

Given Abl's well-known role as a regulator of actin cytoskeleton dynamics and its extensive colocalization with F-actin throughout photoreceptor development (Fig. 1F&G), we hypothesized that problems in regulating F-actin assembly and organization might contribute to the displacement of the photoreceptor cells in *abl* mutant ommatidia to an aberrantly basal position within the epithelium. To test this, we examined the organization of F-actin in photoreceptor cells at third instar and 24hr APF. In third instar eye discs, the overall pattern of phalloidin staining appears comparable between wild-type and *abl* mutant tissue, with normal F-actin enrichment at the apical tips of the photoreceptor cells (Fig. 5A). At 24hr APF, about ten hours before the initiation of rhabdomere formation (Cagan and Ready, 1989), phalloidin staining remains largely normal in *abl* mutant clones, although a modest disruption to the regularity of the ommatidial pattern becomes apparent (Fig. 5B). This apparently normal F-actin organization leads us to suggest that the primary consequence of *abl* loss is a delay in assembling appropriate protein complexes at the specialized AJs and apical membrane, which then leads to the photoreceptors failing to assume or maintain a normal apicobasal position within the epithelium.

Rhabdomeres fail to generate in *abl* mutant photoreceptors

Besides being an integral part of the cytoskeleton, F-actin is also a major structural component of the rhabdomere, the light-sensing organelle of the photoreceptor cells. In a wild-type 48hr APF ommatidium, the first microvillar extensions of the forming rhabdomeres can be detected at the apical surface of the photoreceptor cells as an intense F-actin concentration in the center of each ommatidium (Fig. 5C). In contrast, this F-actin accumulation drastically reduced or absent in *abl* mutant ommatidia (Fig. 5C and Supp. Fig. 4A, B). Unlike Arm or the other apical markers we examined (Figs. 2 and 3), F-actin accumulation is not observed in more basal planes of the retina. Extending the analysis to 72hr and 96hr APF shows the continued absence of rhabdomeric structures in *abl* mutant clones (Fig. 5D&E). These results suggest the program of apical membrane specialization underlying rhabdomere biogenesis fails to initiate in *abl* mutant ommatidia, and are consistent with histological analysis of the adult eye which reveals a complete loss of ommatidial organization such that few, if any, *abl* mutant rhabdomeres are present (Henkemeyer et al., 1987 and Fig. 2F, G).

abl* function in photoreceptor morphogenesis may be independent of *enabled

Both in the context of embryonic CNS axon guidance and during epithelial morphogenesis, the Abl kinase negatively regulates the activities of its substrate Enabled (Ena), an actin regulator (Grevengoed et al., 2001; Grevengoed et al., 2003; Fox and Peifer, 2007). In the contexts of embryonic dorsal closure and ventral furrow formation, loss of *abl* alters Ena localization such that it becomes unevenly distributed with some ectopic accumulation (Grevengoed et al., 2001; Gates et al., 2007). This led us to examine the consequences of *abl* loss on localization of Ena in the photoreceptor cells. In wild-type third instar larval eye

tissue, Ena is enriched at the apical junctional region of the differentiating photoreceptor cells (Grevengoed et al., 2001) and Fig. 6A). Loss of *abl* appears to have no effect on the level or distribution of Ena (Fig. 6A). At 24hr APF, in either wild-type or *abl* mutant ommatidia, Ena becomes enriched at the apical membranes of the photoreceptors and less concentrated at the basolateral membranes (Fig. 6B&C). At 48hr APF, Ena localizes apically to the center of each wild-type ommatidial cluster, but collapses to the basal plane of the epithelium in *abl* mutant ommatidia (Fig. 6D&E). Given that Arm and the apical membrane markers show a similar collapse, the altered Ena localization probably reflects the defects in photoreceptor spatial organization, rather than a specific disruption to Ena distribution.

We also examined the consequences of reducing *ena* dosage on the photoreceptor morphogenetic defects caused by loss of *abl*. If *ena* is required for *abl* function, then reducing *ena* dose might dominantly suppress the *abl* loss-of-function phenotypes, as has been shown in other developmental contexts (Gertler et al., 1995; Grevengoed et al., 2003b). In third instar discs, we find weak enrichment of Arm and aPKC in *ena^{GCI/+}; abl²* mutant clones, just as in *abl²* clones alone (Fig. 2A, 3A, 6F&G). We also examined the apical-basal positions of mutant photoreceptors at 48hr APF, and found no obvious difference between *abl²* and *ena^{GCI/+}; abl²* clones (Fig. 4C and 6H). Quantification of 42 mutant ommatidia in 4 independent *ena^{GCI/+}; abl²* discs revealed 1.6 remaining apical Elav-positive nuclei per ommatidium, a result identical to that obtained for *abl* alone. Similarly, reducing *ena* dose does not restore rhabdomeric structures at 48hr APF, as F-actin accumulation in the center of the *ena^{GCI/+}; abl²* clusters (Fig. 6I) remains dramatically reduced relative to adjacent wild-type ommatidia. While we cannot rule out the possibility that Ena levels are not limiting in the eye as they appear to be in the embryo, the lack of genetic suppression in this experiment, when considered together with the fact that loss of *abl* does not perturb Ena localization, suggests Abl function in these aspects of photoreceptor morphogenesis may be less dependent on Ena than it is in the embryo.

Discussion

In this study, we show that loss of *abl* impairs multiple aspects of photoreceptor morphogenesis, including specialization and remodeling of the AJs and apical membrane domain, rhabdomere generation and spatial organization of cells along the apical-basal axis of the epithelium. In contrast to previously documented roles for *abl-ena* interactions during embryonic epithelial morphogenesis, our results suggest a less prominent role for Ena in transducing Abl-mediated signals during photoreceptor morphogenesis. The fact that such profound morphogenetic defects result from loss of *abl* suggests the Abl tyrosine kinase plays essential and central roles in coordinating upstream signaling inputs with cytoskeleton dynamics to organize the physical architecture of the developing photoreceptors.

What is the primary consequence of *abl* loss in the photoreceptors? The absence of obvious defects in F-actin organization in *abl* mutant photoreceptors in the larval and early pupal discs suggests it is not altered actin cytoskeleton dynamics. Rather, reduced accumulation of Arm in the AJs and of aPKC, Crumbs and PATJ at the apical membrane is evident in the photoreceptor cells shortly after they emerge from the morphogenetic furrow. Considering both how tightly these two phenotypes appear linked in developmental time and the fact that endogenous Abl protein localization in the apical-junctional domain overlaps with both sets of markers in the third instar discs, the two defects likely reflect independent functional requirements for *abl* rather than one being a secondary consequence of the other.

Prior analyses of retinal phenotypes resulting from loss of either AJ or apical protein complex components support the idea of parallel independent development of these

structures in the young photoreceptors. For example, loss of apical complex components such as Crumbs, Bazooka or Stardust does not perturb establishment of the AJs and apicobasal polarity of the larval photoreceptors (Pellikka et al., 2002; Hong et al., 2003). Conversely, loss of *shotgun*, the gene encoding the AJ component E-cadherin, disrupts junctional Arm localization and leads to defects in planar cell polarity (PCP) (Mirkovic and Mlodzik, 2006), but to our knowledge has not been shown to disrupt the apical complex in the early photoreceptors. Recently, *abl* has itself been implicated in PCP in the eye (Singh et al., 2010), suggesting its role in stabilizing the AJs may be critical for subsequent transmission and integration of the signaling pathways that regulate PCP. Thus individual disruption of either the AJ or apical domain complex proteins appears insufficient to phenocopy *abl* loss, arguing for independent functional requirements for *abl* in each.

The failure of *abl* mutant photoreceptors to maintain their normal apical-basal position within the epithelium likely results as a consequence of the initial defects in the AJs and apical domain. Some basal displacement of apical/junctional markers and nuclei is already evident in third instar and 24hr APF *abl* mutant photoreceptors, suggesting that the cells may be slightly less elongated than their wild-type counterparts. By 48hr APF, a stage marked by rapid deepening of the retinal epithelium, the inappropriate basal position of both apical/junctional proteins and photoreceptor nuclei becomes strikingly evident in *abl* mutant ommatidia. However, although basally displaced, the *abl* mutant photoreceptors maintain fairly normal accumulation of AJ and apical domain markers at 48hr APF. This suggests that although *abl* is required for the efficient initial enrichment of apical-junctional protein complexes in the young photoreceptors, the system can compensate for the delay and essentially normal complexes eventually accumulate and are maintained in pupal *abl* mutant photoreceptors. However the initial delay may compromise critical cell-cell interactions, effectively weakening cell contacts such that the *abl* mutant photoreceptors are unable to maintain their normal position within the epithelium as they elongate. Perhaps the nonautonomous rescue observed in mosaic ommatidia results from stronger cell-cell interactions provided by the wild-type cells physically supporting the *abl* mutant photoreceptors.

Finally, the initial defects in the AJs and apical domain, as well as the apicobasal disorganization, likely contribute synergistically to the subsequent failure of *abl* mutant photoreceptors to initiate rhabdomere formation. In wild-type animals, coordinated expansion and remodeling of the photoreceptor apical membrane drives formation of the rhabdomeres, and both the AJs and apical complex proteins appear critical to the process. For example, loss of *crumbs* compromises integrity of the expanding AJs, resulting in incomplete rhabdomere extension and subsequent collapse and fragmentation (Izaddoost et al., 2002; Pellikka et al., 2002). Loss of *abl* results in a more severe phenotype, namely failure to initiate rhabdomere formation, presumably reflecting the fact that both the AJs and apical membrane domains are compromised. Given Abl's well-documented ability to regulate the actin cytoskeleton during embryonic epithelial and neuronal morphogenesis, its tight colocalization with F-actin at 48hr APF suggests it may also have a primary role in assembling the actin-based rhabdomeres. Consistent with this hypothesis, although we observe normal AJs and apicobasal position of *abl* mutant cells in mosaic ommatidia at 48hr APF, we rarely find any rhabdomeres in *abl* mutant cells in adult sections, even in mosaic ommatidia. Thus Abl may be involved in assembling and/or maintaining the actin-based rhabdomere structures, independent of its earlier functions in elaborating the apical-junctional domains.

What are the molecular mechanisms underlying the prominent functions of Abl in photoreceptor morphogenesis? Abl regulates *Drosophila* embryonic epithelial morphogenesis and axon guidance in part by regulating the localization of Enabled (Gertler

et al., 1990; Grevenkoed et al., 2001; Grevenkoed et al., 2003). However, unlike what has been observed in these developmental contexts, reducing *enabled* dosage does not suppress the severity of the AJ and apical membrane domain defects seen in *abl* mutant photoreceptors. While this could simply mean Ena protein amounts are not limiting, the fact that loss of *abl* does not perturb Ena localization leads us to speculate that Abl function in retinal epithelial patterning may depend on downstream effectors other than Enabled.

Previously, our lab has identified the transcription factor/phosphatase Eyes absent (Eya) as a substrate of the Abl tyrosine kinase (Xiong et al., 2009). The fact that Eya and Abl function cooperatively in the context of photoreceptor axon targeting (Xiong et al., 2009) prompted us to examine the possibility that Eya might be a downstream effector of Abl in other aspects of photoreceptor morphogenesis. However, unlike the axon guidance context, where heterozygosity for *eya* dominantly enhances *abl* phenotypes (Xiong et al., 2009), reducing *eya* gene dosage does not modify the *abl* clone phenotypes we report here (data not shown). This suggests that Eya is unlikely to be a downstream effector of Abl in the contexts examined in this paper.

Other candidates might include the guanine nucleotide exchange factor Trio, which may link Abl to the Rho family small GTPases to control cell morphology during embryogenesis (Liebl et al., 2000b; Forsthoefel et al., 2005), and the tyrosine-phosphorylated adaptor protein Disabled (Dab), a component of the Abl signaling pathway that has recently been shown to be required for proper subcellular distribution of Abl in the eye disc epithelium (Gertler et al., 1989; Gertler et al., 1993; Song et al., 2010). However, because *trio* mutant photoreceptors have no other disruptions in differentiation or morphogenesis other than axon guidance defects (Newsome et al., 2000b), and Dab functions upstream of Abl (Song et al., 2010), neither protein would seem a likely downstream Abl pathway effector in the contexts examined in this paper. Thus identifying the signaling pathways and complexes with which Abl interacts in the AJs and apical membrane domain will be required to reveal the signaling mechanisms used by Abl to influence retinal epithelial morphogenesis.

Experimental Procedures

Fly genetics

The amorphic allele *abl*² and strong hypomorphic allele *abl*¹ (Henkemeyer et al., 1987) were recombined onto the *FRT80B* chromosome. Homozygous *abl* mutant eye clones in wild-type or *enabled* heterozygous background were generated using the *ey-FLP/FRT* system. *abl*²*FRT80B/TM6Tubby* or *ena*^{GCl}/*CyoGFP*; *abl*²*FRT80B/TM3GFP* males were crossed to *ey-FLP*; *GFPnlsFRT80B* virgins, and non-tubby/GFP third instar larvae or pre-pupae were collected. *abl*²/*TM6Tubby*, *ena*^{GCl}/*Cyo* and *ey-FLP*; *GFPnlsFRT80B* fly stocks were obtained from the Bloomington stock center.

Collecting and aging pupae

The genotyped immobile white pre-pupae were collected and grown in a humid chamber at 25°C. Pupae were harvested at 24hr, 48hr, 72hr and 96hr time points for dissections.

Immunostaining and antibodies

Late third instar larval, 24 or 48hr APF eye discs were dissected in S2 cell medium (Gibco, sf-900 II SFM) and fixed for 10 minutes in 4% paraformaldehyde in PBS with 0.1% Triton X-100 at room temperature. For 72 and 96hr pupal and adult eye dissections, heads were cut in half, fixed for 20 minutes at room temperature prior to dissecting the eye tissue and fixing again for 10 minutes at room temperature. Fixed tissues were washed 3× in PBT (PBS with 0.1% Triton X-100), blocked in PNT (PBS with 0.1% Triton X-100 and 3% normal goat

serum) for 1hr at room temperature, incubated overnight at 4°C in primary antibodies diluted in PNT, washed 3× in PBT, incubated in secondary antibodies diluted in PNT for 2hr at room temperature, washed 3× in PBT, mounted in antifade mounting solution (Invitrogen, ProLong® Antifade Kit), and imaged on a Zeiss 510 confocal microscope. The antibodies used in this study were mouse anti-Elav, anti-Ena, anti-Armadillo, anti-Chaoptin, anti-Crumbs (1:1000) (all used as 1:10 if not otherwise indicated, Developmental Studies Hybridoma Bank); rat anti-Abl (1:500, gift from D. Van Vactor), guinea pig anti-So (1:2000), rabbit anti-GFP (1:1000, Invitrogen), rabbit anti-aPKC (1:1000, Santa Cruz), rabbit anti-PATJ (1:20000, (Bhat et al., 1999)), mouse anti-GFP (1:100, Invitrogen), Rho/OG-phalloidin (1:2000, Molecular probes) and Cy3/FITC/Cy5-conjugated secondary antibodies (1:2000, Jackson Immunoresearch).

Histological analysis of adult eyes

Fly heads were severed and bisected in phosphate buffer (0.1M sodium phosphate pH 7.2), transferred immediately to fixing solution (2.5% glutaraldehyde in phosphate buffer) and incubated in a 1:1 mix of fixing solution and 2% OsO₄ in phosphate buffer on ice for 30 min. Eyes were washed 3 times with cold phosphate buffer, incubated with fresh OsO₄ on ice for 2hr, dehydrated on ice by successive 10 min incubations in 30%, 50%, 70%, 90% and 100% ethanol followed by two 10min washes in 100% ethanol and three 10min washes in propylene oxide at room temperature. An equal amount of Durcupan resin was added to the last propylene oxide wash and mixed thoroughly. Eyes were incubated in the mixture overnight at room temperature and embedded in Durcupan resin overnight at 60°C. 1.5 micron-thick eye sections were cut on a microtome, transferred to gelatin-subbed slides and mounted in DPX (Fluka). The bright field picture was taken under a 100X objective using a Zeiss Axioplan 2 microscope.

Supplementary Material

Refer to Web version on PubMed Central for supplementary material.

Acknowledgments

We thank P. Vanderzalm, J. Zhang, S. Morillo, J. Webber and S. Horne-Badovinac for comments on the manuscript, members of the Rebay, Fehon and Horne-Badovinac labs for discussions, M. DiMarco and N. Martin for confocal assistance, and R. Fehon and D. Van Vactor for antibody reagents. We acknowledge the Bloomington *Drosophila* stock centers for flies, and the Developmental Studies Hybridoma Bank for antibodies. This research was supported by National Institutes of Health grant R01 EY12549 to I.R., a Women's Board Fellowship of the University of Chicago and an American Heart Association predoctoral fellowship to W.X..

References

- Bashaw GJ, Kidd T, Murray D, Pawson T, Goodman CS. Repulsive axon guidance: Abelson and Enabled play opposing roles downstream of the roundabout receptor. *Cell*. 2000; 101:703–715. [PubMed: 10892742]
- Bate, M.; Arias, AM., editors. *The Development of Drosophila melanogaster*. Plainview: Cold Spring Harbor Press; 1993. p. 811
- Bennett RL, Hoffmann FM. Increased levels of the *Drosophila* Abelson tyrosine kinase in nerves and muscles: subcellular localization and mutant phenotypes imply a role in cell-cell interactions. *Development*. 1992; 116:953–966. [PubMed: 1295746]
- Bhat MA, Izaddoost S, Lu Y, Cho KO, Choi KW, Bellen HJ. Discs Lost, a novel multi-PDZ domain protein, establishes and maintains epithelial polarity. *Cell*. 1999; 96:833–845. [PubMed: 10102271]
- Cagan RL, Ready DF. The emergence of order in the *Drosophila* pupal retina. *Dev Biol*. 1989; 136:346–362. [PubMed: 2511048]

- Forsthoefel DJ, Liebl EC, Kolodziej PA, Seeger MA. The Abelson tyrosine kinase, the Trio GEF and Enabled interact with the Netrin receptor Frazzled in *Drosophila*. *Development*. 2005; 132:1983–1994. [PubMed: 15790972]
- Fox DT, Peifer M. Abelson kinase (Abl) and RhoGEF2 regulate actin organization during cell constriction in *Drosophila*. *Development*. 2007; 134:567–578. [PubMed: 17202187]
- Gates J, Mahaffey JP, Rogers SL, Emerson M, Rogers EM, Sottile SL, Van Vactor D, Gertler FB, Peifer M. Enabled plays key roles in embryonic epithelial morphogenesis in *Drosophila*. *Development*. 2007; 134:2027–2039. [PubMed: 17507404]
- Gertler FB, Bennett RL, Clark MJ, Hoffmann FM. *Drosophila* abl tyrosine kinase in embryonic CNS axons: a role in axonogenesis is revealed through dosage-sensitive interactions with disabled. *Cell*. 1989; 58:103–113. [PubMed: 2502313]
- Gertler FB, Comer AR, Juang JL, Ahern SM, Clark MJ, Liebl EC, Hoffmann FM. enabled, a dosage-sensitive suppressor of mutations in the *Drosophila* Abl tyrosine kinase, encodes an Abl substrate with SH3 domain-binding properties. *Genes Dev*. 1995; 9:521–533. [PubMed: 7535279]
- Gertler FB, Doctor JS, Hoffmann FM. Genetic suppression of mutations in the *Drosophila* abl proto-oncogene homolog. *Science*. 1990; 248:857–860. [PubMed: 2188361]
- Gertler FB, Hill KK, Clark MJ, Hoffmann FM. Dosage-sensitive modifiers of *Drosophila* abl tyrosine kinase function: prospero, a regulator of axonal outgrowth, and disabled, a novel tyrosine kinase substrate. *Genes Dev*. 1993; 7:441–453. [PubMed: 7680635]
- Gibson MC, Perrimon N. Apicobasal polarization: epithelial form and function. *Curr Opin Cell Biol*. 2003; 15:747–752. [PubMed: 14644201]
- Grevengoed EE, Fox DT, Gates J, Peifer M. Balancing different types of actin polymerization at distinct sites: roles for Abelson kinase and Enabled. *J Cell Biol*. 2003; 163:1267–1279. [PubMed: 14676307]
- Grevengoed EE, Loureiro JJ, Jesse TL, Peifer M. Abelson kinase regulates epithelial morphogenesis in *Drosophila*. *J Cell Biol*. 2001; 155:1185–1198. [PubMed: 11756472]
- Hayashi T, Carthew RW. Surface mechanics mediate pattern formation in the developing retina. *Nature*. 2004; 431:647–652. [PubMed: 15470418]
- Henkemeyer MJ, Gertler FB, Goodman W, Hoffmann FM. The *Drosophila* Abelson proto-oncogene homolog: identification of mutant alleles that have pleiotropic effects late in development. *Cell*. 1987; 51:821–828. [PubMed: 3119227]
- Hernandez SE, Krishnaswami M, Miller AL, Koleske AJ. How do Abl family kinases regulate cell shape and movement? *Trends Cell Biol*. 2004; 14:36–44. [PubMed: 14729179]
- Hong Y, Ackerman L, Jan LY, Jan YN. Distinct roles of Bazooka and Stardust in the specification of *Drosophila* photoreceptor membrane architecture. *Proc Natl Acad Sci U S A*. 2003; 100:12712–12717. [PubMed: 14569003]
- Izaddoost S, Nam SC, Bhat MA, Bellen HJ, Choi KW. *Drosophila* Crumbs is a positional cue in photoreceptor adherens junctions and rhabdomeres. *Nature*. 2002; 416:178–183. [PubMed: 11850624]
- Kumar JP, Moses K. Cell fate specification in the *Drosophila* retina. *Results Probl Cell Differ*. 2000; 31:93–114. [PubMed: 10929403]
- Liebl EC, Forsthoefel DJ, Franco LS, Sample SH, Hess JE, Cowger JA, Chandler MP, Shupert AM, Seeger MA. Dosage-sensitive, reciprocal genetic interactions between the Abl tyrosine kinase and the putative GEF trio reveal trio's role in axon pathfinding. *Neuron*. 2000; 26:107–118. [PubMed: 10798396]
- Longley RL Jr, Ready DF. Integrins and the development of three-dimensional structure in the *Drosophila* compound eye. *Dev Biol*. 1995; 171:415–433. [PubMed: 7556924]
- Mirkovic I, Mlodzik M. Cooperative activities of *drosophila* DE-cadherin and DN-cadherin regulate the cell motility process of ommatidial rotation. *Development*. 2006; 133:3283–3293. [PubMed: 16887833]
- Newsome TP, Asling B, Dickson BJ. Analysis of *Drosophila* photoreceptor axon guidance in eye-specific mosaics. *Development*. 2000a; 127:851–860. [PubMed: 10648243]

- Newsome TP, Schmidt S, Dietzl G, Keleman K, Asling B, Debant A, Dickson BJ. Trio combines with dock to regulate Pak activity during photoreceptor axon pathfinding in *Drosophila*. *Cell*. 2000b; 101:283–294. [PubMed: 10847683]
- Pelikka M, Tanentzapf G, Pinto M, Smith C, McGlade CJ, Ready DF, Tepass U. Crumbs, the *Drosophila* homologue of human CRB1/RP12, is essential for photoreceptor morphogenesis. *Nature*. 2002; 416:143–149. [PubMed: 11850625]
- Ready DF, Hanson TE, Benzer S. Development of the *Drosophila* retina, a neurocrystalline lattice. *Dev Biol*. 1976; 53:217–240. [PubMed: 825400]
- Singh J, Yanfeng WA, Grumolato L, Aaronson SA, Mlodzik M. Abelson family kinases regulate Frizzled planar cell polarity signaling via Dsh phosphorylation. *Genes Dev*. 2010; 24:2157–2168. [PubMed: 20837657]
- Song JK, Kannan R, Merdes G, Singh J, Mlodzik M, Giniger E. Disabled is a bona fide component of the Abl signaling network. *Development*. 2010; 137:3719–3727. [PubMed: 20940230]
- Tepass U, Harris KP. Adherens junctions in *Drosophila* retinal morphogenesis. *Trends Cell Biol*. 2007; 17:26–35. [PubMed: 17134901]
- Tomlinson A. The cellular dynamics of pattern formation in the eye of *Drosophila*. *J Embryol Exp Morphol*. 1985; 89:313–331. [PubMed: 3937883]
- Tomlinson A, Ready DF. Neuronal differentiation in *Drosophila* ommatidium. *Dev Biol*. 1987; 120:366–376. [PubMed: 17985475]
- Xiong W, Dabbouseh NM, Rebay I. Interactions with the abelson tyrosine kinase reveal compartmentalization of eyes absent function between nucleus and cytoplasm. *Dev Cell*. 2009; 16:271–279. [PubMed: 19217428]

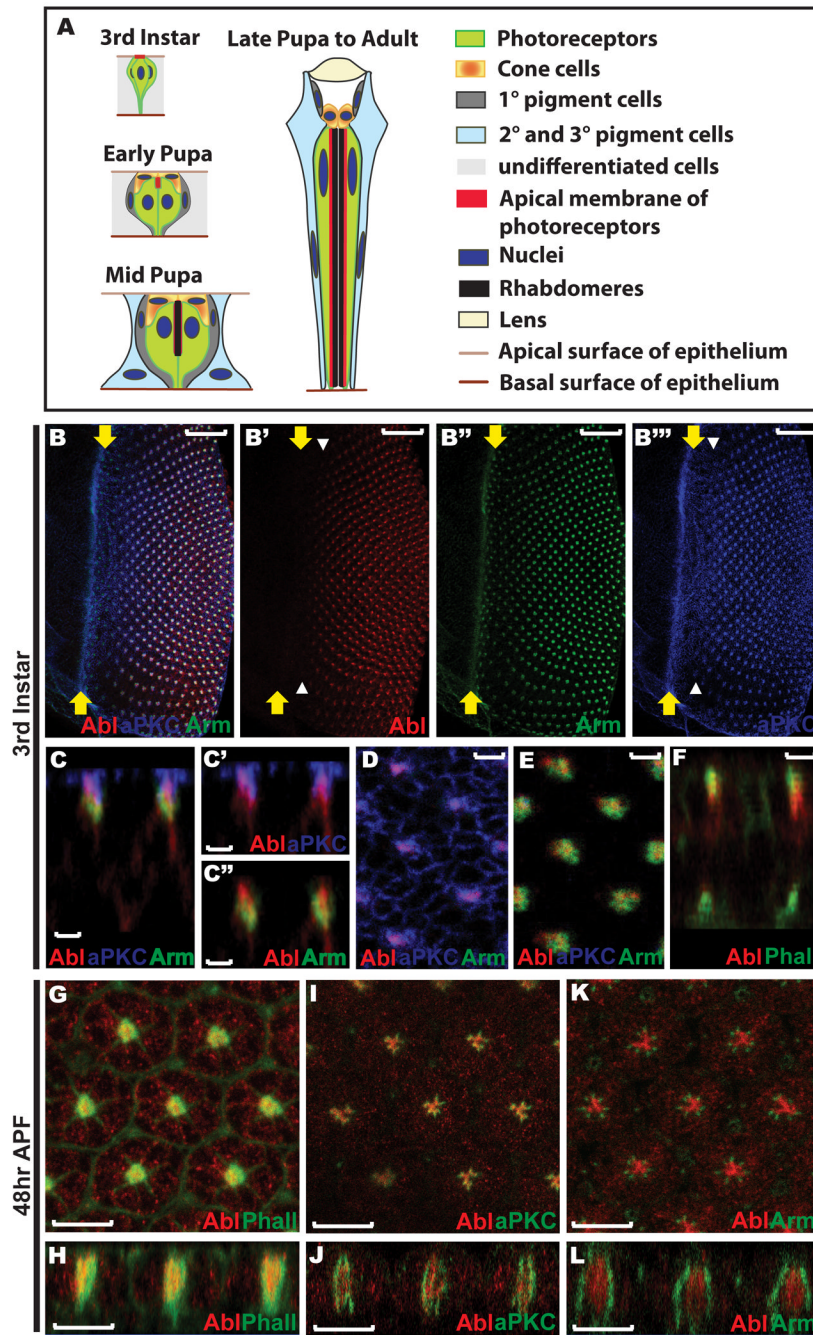


Figure 1. Abl protein localization in the developing eye disc

A) A schematic summarizing the major morphogenetic events during *Drosophila* ommatidial development. In the third instar larval eye disc the newly specified photoreceptor cells display a similar apical-basal polarity to that of other cells in the epithelium. By the early pupal stage, the apical membrane of each photoreceptor has turned 90° towards the center of its cluster and detached from the apical surface of the epithelium, with the four newly specified cone cells covering the apical space left by the involution of the photoreceptor apical membranes. During mid-pupal stages, rhabdomeres are assembled at the apex of the elongating apical membranes of the photoreceptors. Both the photoreceptor apical membranes and the rod-like rhabdomeres continue to extend basally as

all cells in the epithelium elongate. By 90hr APF, shortly before eclosion to the adult, the final ommatidial organization has been achieved: eight photoreceptor cells with rod-like rhabdomeres occupy the center of each ommatidium, with four cone cells surrounding and capping them and eleven pigment cells forming two outer whorls. Figures are not drawn to scale and were adapted from (Bate and Arias, 1993, Chapter 22, Figure 2) and from (Tepass and Harris, 2007).

B) A maximum confocal projection of all transverse sections crossing a wild type third instar larval eye disc stained with anti-Abl (red, B'), anti-Arm (green, B''), and anti-aPKC (blue, B'''). Abl expression initiates a few rows posterior to the furrow, coincident with the onset of aPKC enrichment at the constricting apical membrane of the developing photoreceptors (white arrowheads, B' & B'''). All third instar larval eye discs shown in this paper are oriented with anterior left, dorsal up, and position of the morphogenetic furrow marked with yellow arrows. Scale bars: 20 μm .

C) An orthogonal section of the disc shown in (B) shows the extent of overlap of Abl with aPKC (C') and Arm (C'') along the apical-basal axis. All orthogonal sections shown in this paper are oriented with apical up and basal down. Scale bars: 2 μm .

D-E) Zoomed-in views of single transverse sections crossing the most apical (D) and subapical (E) regions of the disc shown in (B). Scale bars: 2 μm .

D) Abl colocalizes with aPKC at the apical domain of the photoreceptors at the center of each developing cluster, but is absent from the apical membranes of the undifferentiated epithelial cells where aPKC is expressed.

E) Abl overlaps with Arm at the AJs of the photoreceptor clusters.

F) An orthogonal section of a wild-type third instar larval eye disc stained with anti-Abl (red) antibody and OG-Phalloidin (green) shows colocalization of Abl with actin filaments at the apical region. Scale bars: 2 μm .

G-L) 48hr APF wild-type eye discs stained with anti-Abl (red) and OG-Phalloidin (green, G-H), anti-aPKC (green, I-J) or anti-Arm (green, K-L) antibodies. G, I, K) are the face views and H, J, L) are the orthogonal sections. Scale bars: 10 μm .

G-H) A single middle section showing Abl colocalization with F-actin in the center of each ommatidium.

I-J) A single middle section showing Abl partially overlaps with aPKC at the apical surface of the photoreceptor cells, but that most Abl protein localizes to the center of each ommatidium where no aPKC is observed.

K-L) A single middle section showing Abl does not overlap with Arm at this stage.

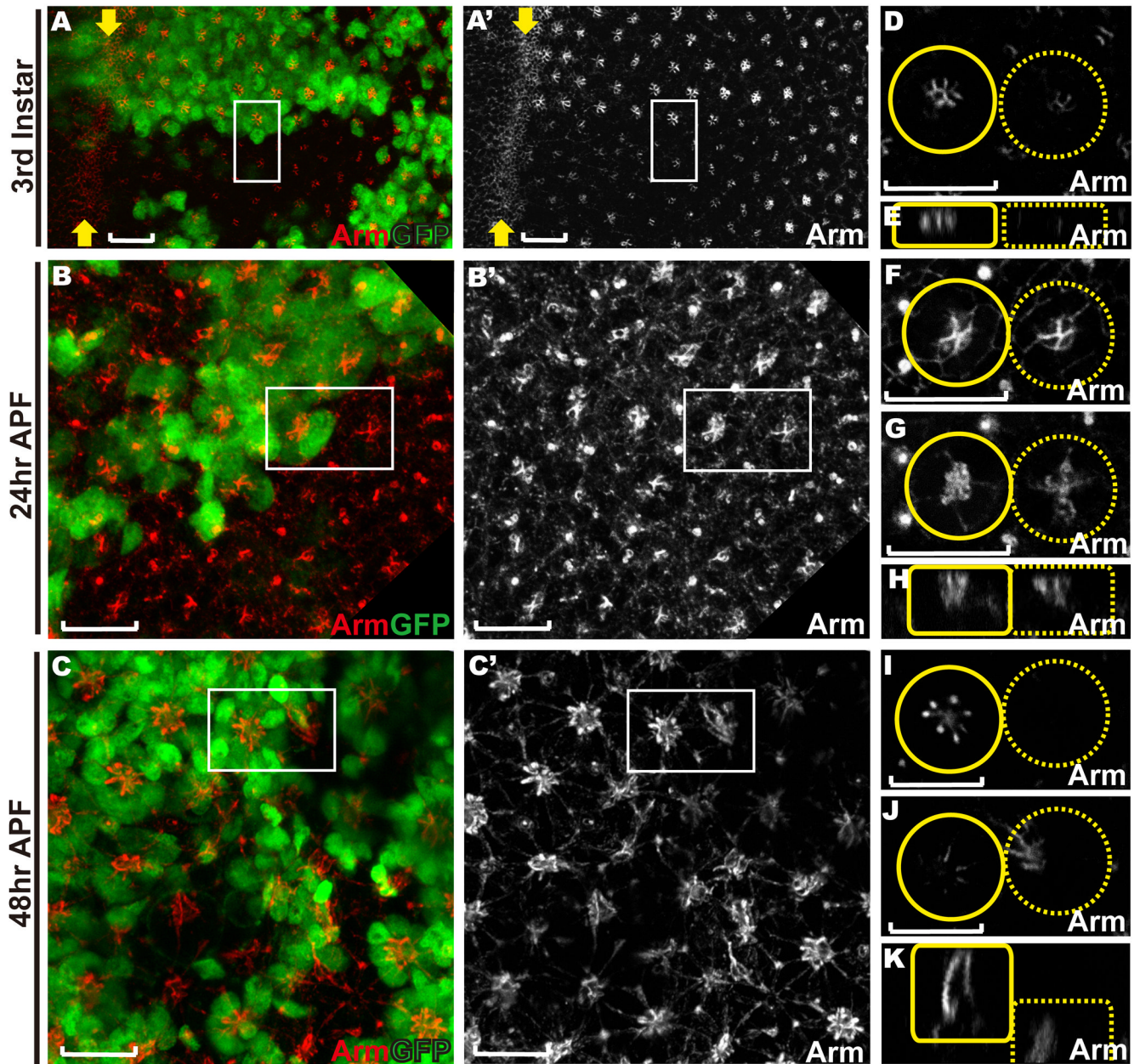


Figure 2. Loss of *abl* delays and disrupts the organization of adherens junctions between the photoreceptors

Eye discs with *abl* clones were stained with anti-Arm (red) and anti-GFP (green) antibodies. Lack of GFP marks *abl* mutant clones in this and all other figures in this paper. Scale bars: 10 μ m.

A-C) are confocal projections of all transverse sections, and D-K) are zoomed-in single transverse (D, F-G, I-J) or orthogonal (E, H, K) sections of the two adjacent ommatidia (outlined by white boxes in A-C) with the wild-type ommatidium outlined by a solid yellow circle/box and the *abl* mutant ommatidium outlined by a dashed yellow circle/box.

A, D-E) Arm expression appears reduced, but fairly normally patterned and localized in *abl* mutant ommatidia in a third instar disc.

B, F-H) At 24hr APF, the adherens junctions between the cone cells in *abl* mutant ommatidia appear normal (F). Arm enrichment between the *abl* mutant photoreceptor cells is clearly evident at this stage, although still mildly weaker and less tightly organized than wild type (G).

C, I-K) At 48hr APF, apical Arm enrichment is undetectable in *abl* mutant ommatidia (I) and has collapsed to the basal plane of the epithelium (J-K).

Supplementary Fig. 2 shows analogous phenotypes in the hypomorphic *abl^l* allele.

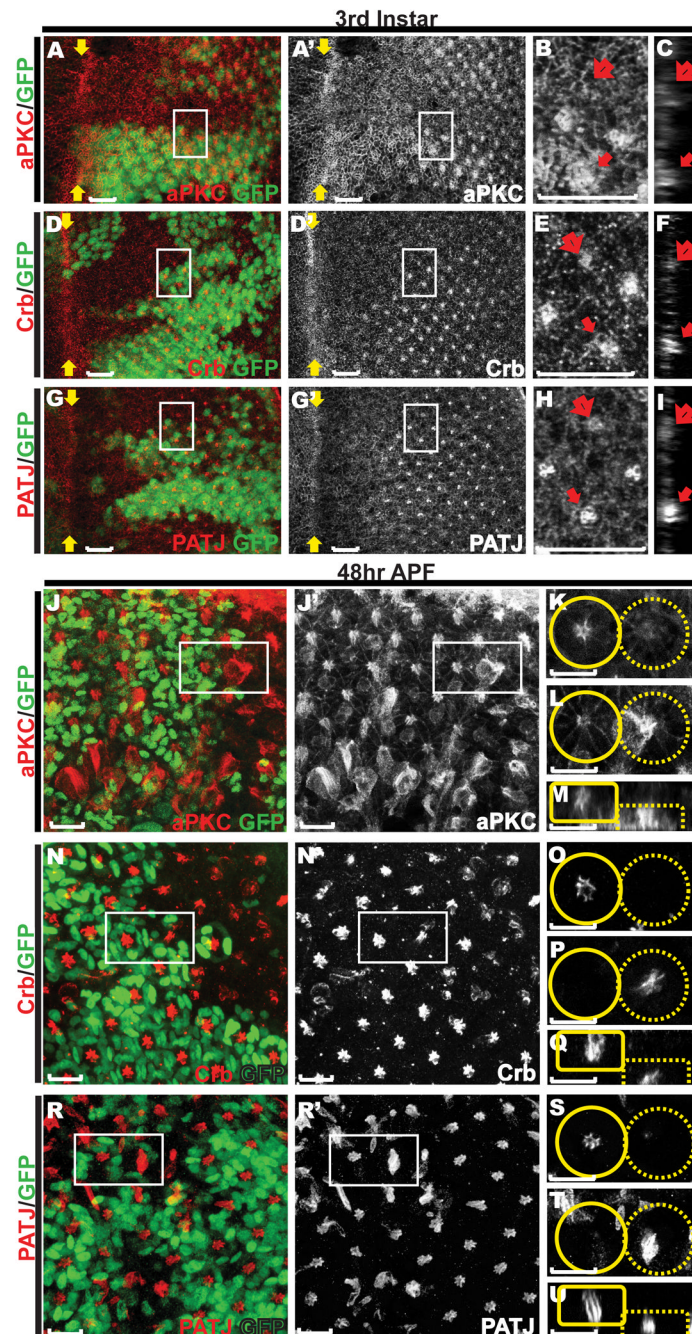


Figure 3. Defects in organization of the apical membrane domains in *abl* mutant ommatidial clusters

Eye discs carrying *abl* mutant clones stained with anti-GFP (green) and either anti-aPKC (red, A-C, J-M), anti-Crumbs (red, D-F, N-Q), or anti-PATJ (red, G-I, R-U). Scale bars: 10 μ m. A, D, G are maximum projection confocal images of third instar discs, with zoomed-in views (B, E, H, outlined by white boxes in A, D and G) and orthogonal sections of the zoomed-in regions (C, F and I). The enrichment of all three apical membrane markers in the center of *abl* mutant ommatidium (open arrows in B-C, E-F, H-I) is reduced compared to that of wild-type ommatidia (solid arrows in B-C, E-F, H-I).

J, N, R) are maximum projection confocal images of 48hr APF discs with zoomed-in single transverse (K-L, O-P, S-T, outlined by white boxes in J, N and R) or orthogonal (M, Q, U) sections of adjacent wild-type (solid circles/boxes) and *abl* mutant (dashed circles/boxes) ommatidia. Enrichment of all three apical markers in the center of *abl* mutant ommatidial clusters is evident although the structures are disorganized and have collapsed basally.

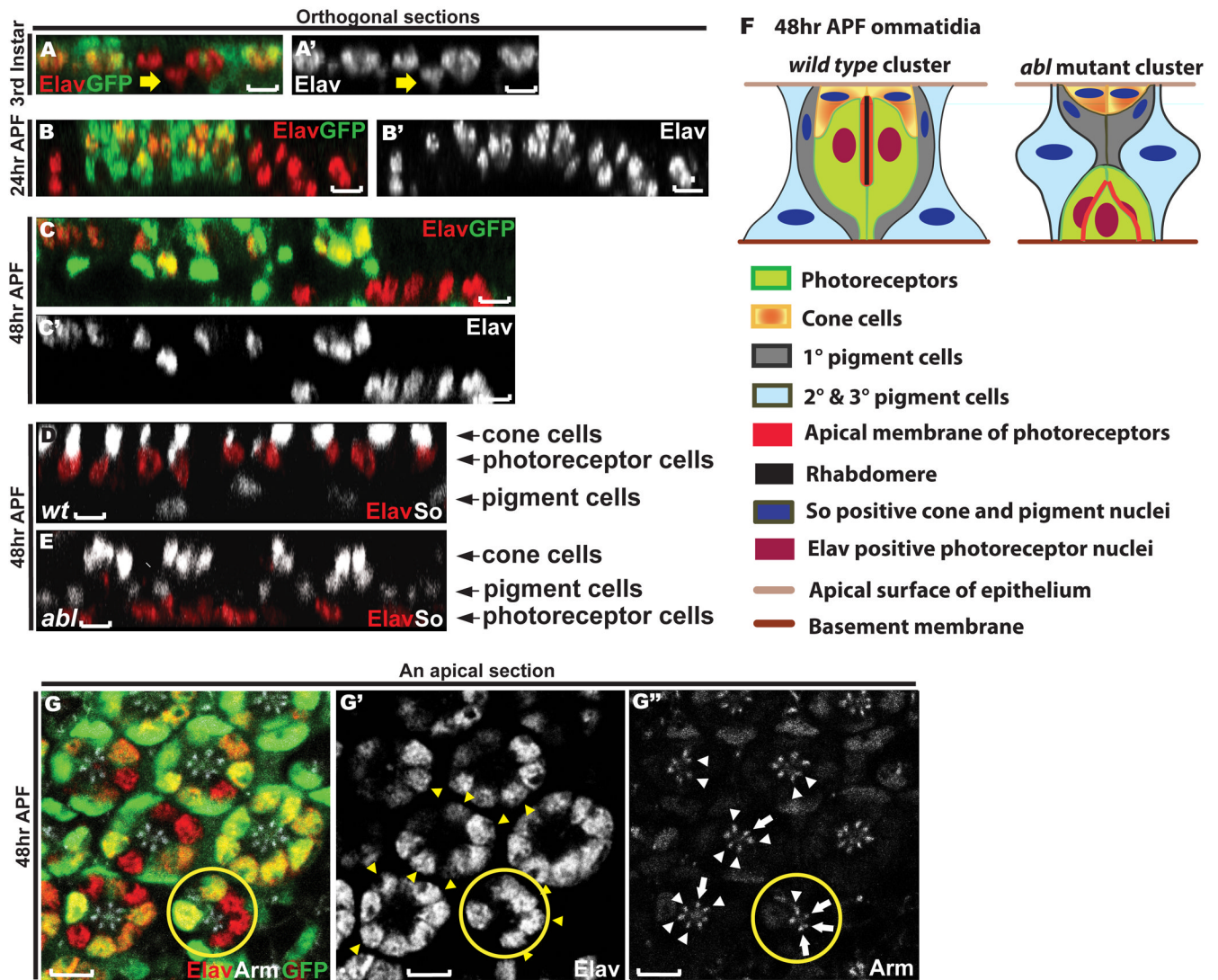


Figure 4. Loss of *abl* disrupts photoreceptor apicobasal positioning

A-E) Orthogonal sections through third instar (A), 24hr APF (B) and 48hr APF (C-E) eye discs. Scale bars: 5 μ m.

A-C) Eye discs with *abl* clones were stained with anti-Elav (red) and anti-GFP (green) antibodies.

A) *abl* mutant photoreceptor cell nuclei (yellow arrow) reside slightly basal relative to wild type.

B-C) At 24hr APF and 48hr APF, this phenotype becomes more apparent.

D-E) Eye discs with wild-type (D) and *abl* mutant (E) clones were stained with anti-Elav (red) and anti-So (green) antibodies. Wild-type and *abl* mutant tissues were distinguished by the presence or absence of GFP (not shown).

D) A wild-type clone showing the normal apical to basal arrangement of cone cell, photoreceptor cell and pigment cell nuclei.

E) In *abl* mutant clones, the Elav positive photoreceptor nuclei are found basal to the pigment cell nuclei.

F) A schematic diagram summarizing the disrupted apical-basal architecture of *abl* mutant ommatidial clusters.

G) A single apical section through a 48hr APF eye disc stained with anti-Elav (red, G'), anti-Arm (white, G'') and anti-GFP (green) antibodies. The nuclei of the *abl* mutant cells (yellow arrowheads in G') in the mosaic ommatidia reside normally at the apical plane of the epithelium, and the AJs between the *abl* mutant cells (white arrows) and those between the *abl* mutant cell and their wild-type neighbor (white arrowheads) appear normal. A mosaic ommatidium with three adjacent *abl* mutant photoreceptors with normally positioned nuclei is outlined by the yellow circle. Scale bars: 5 μ m.

Supplementary Fig. 3 shows apical-basal photoreceptor nuclear position is similarly disrupted in the hypomorphic *abl^l* allele.

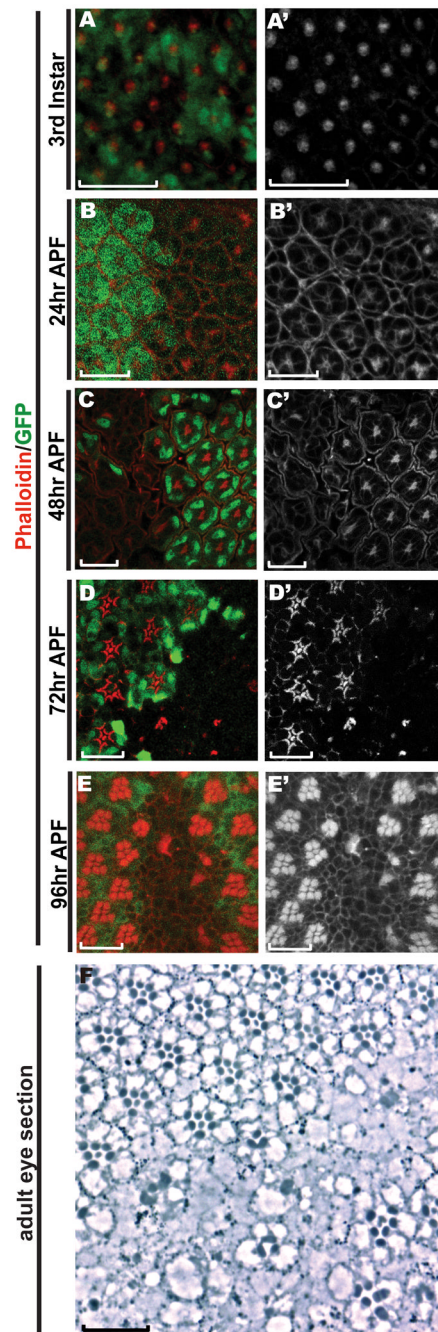


Figure 5. Rhabdomeres fail to generate in *abl* clones

A-E) All eye imaginal discs were stained with Rhodamine-phalloidin (red) and anti-GFP (green). All panels are single transverse sections. Scale bars: 10 μ m.

A) In the third instar disc, F-actin appears normally distributed in *abl* clones.

B) At 24hr APF, F-actin appears normal in *abl* clones, despite the disrupted organization of the mutant ommatidia.

C) At 48hr APF, the central enrichment of F-actin at the microvillar extensions in wild-type tissue is absent in *abl* mutant tissue.

D) At 72hr APF, the expanding rhabdomeres in each wild-type ommatidium are absent in *abl* mutant clones.

E) At 96hr APF, no rhabdomeres are detected in *abl* clones.

F) A histological section of an adult eye shows the lack of rhabdomeres and ommatidial organization in *abl* clones, which are marked by the absence of the product of the *white* gene. The few rhabdomeres seen in the center of the mutant clone actually belong to wild-type cells, as pigment granules can be detected in their cell bodies. Scale bar: 10 μm .

Supplementary Fig. 5 shows analogous defects in F-actin and loss of rhabdomeres in the hypomorphic *abl^l* allele.

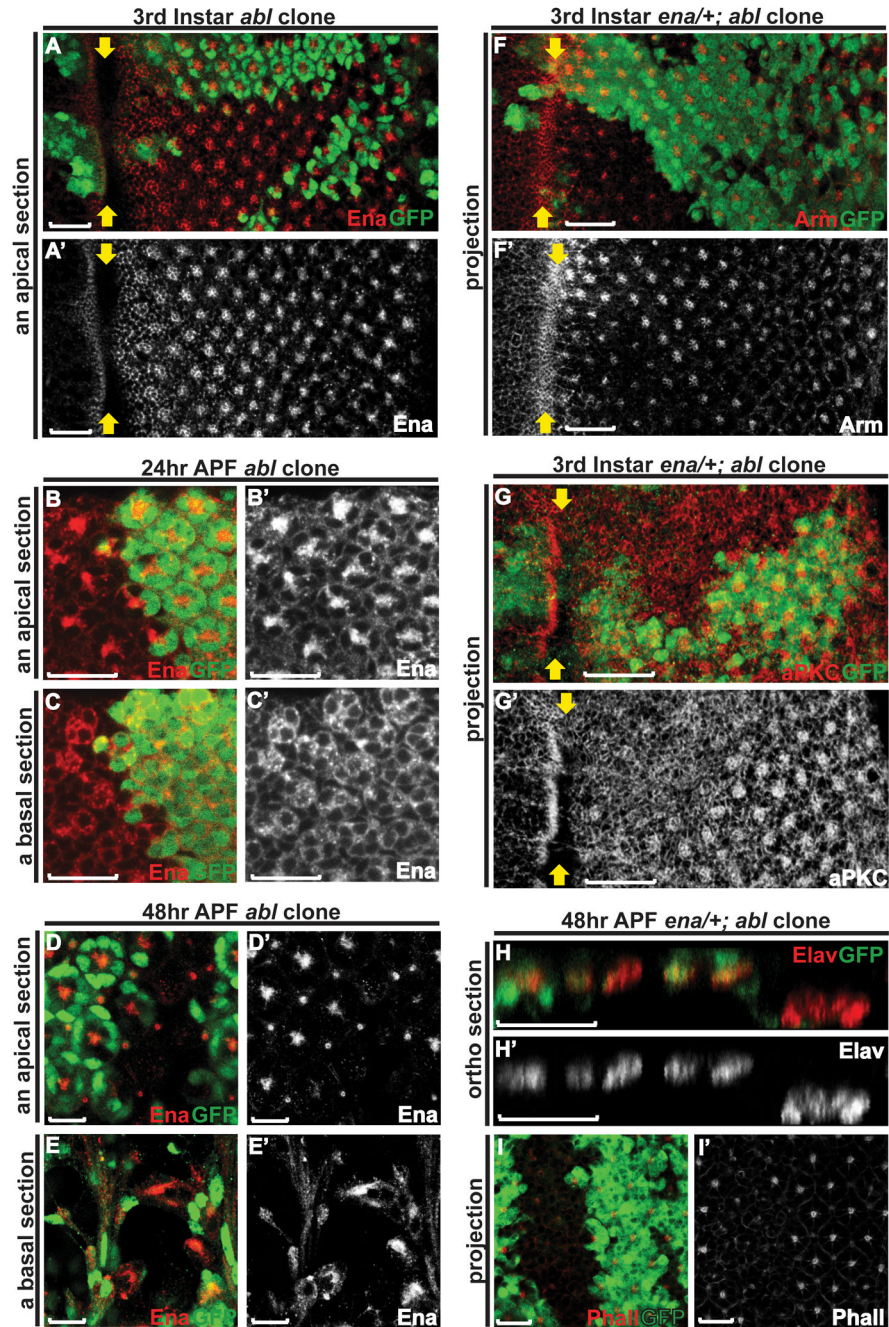


Figure 6. *abl* function during photoreceptor polarity establishment may be independent of *enabled*

A-E) Single transverse sections of eye discs with *abl* clones stained with anti-Enabled (red) and anti-GFP (green) antibodies. Scale bars: 10 μ m.

A) Enabled staining looks normal in the third instar *abl* clones.

B-C) At 24hr APF, the enrichment of Enabled at the apical membrane (B) and its localization to the basal-lateral membrane (C) appears comparable between wild-type and *abl* mutant ommatidia.

D-E) At 48hr APF, Enabled expression is detected basally in *abl* mutant clones, presumably reflecting the disrupted apical-basal positioning of the photoreceptor cells.

F-G) Confocal projections of third instar eye discs with *ena^{GCl/+}; abl* clones were stained with anti-GFP (green) and either anti-Arm (red, F) or anti-aPKC (red, G) antibodies. Arm and aPKC staining is weaker in the *ena^{GCl/+}; abl* clones relative to wild-type, but comparable to that seen *abl* clones as shown in Figures 2A and 3A. Scale bars: 10 μ m.

H) An orthogonal section through a 48hr APF eye disc stained with anti-Elav (red) and anti-GFP antibodies. In the *ena^{GCl/+}; abl* clones, the nuclei of the mutant photoreceptor cells reside at the basal plane of the epithelium, a phenotype similar to that of *abl* clones.

I) Confocal projection of a 48hr APF eye disc stained with Rh-Phalloidin (red) and anti-GFP (green) antibody. F-actin accumulation at the center of the *ena^{GCl/+}; abl* ommatidia remains greatly reduced relative to wild type.